IEEE Access
Multidisciplinary | Rapid Review | Open Access Journal

Date of publication xxxx 00, 0000, date of current version xxxx 00, 0000.

Digital Object Identifier 10.1109/ACCESS.2017.DOI

Balanced-to-Balanced Microstrip Diplexer Based on Magnetically Coupled Resonators

ARMANDO FERNÁNDEZ-PRIETO[1], (Member, IEEE), AINTZANE LUJAMBIO[2], JESÚS MARTEL[3], (Senior Member, IEEE), FRANCISCO MEDINA[1], (Fellow, IEEE), FERRAN MARTÍN[4], (Fellow, IEEE) and RAFAEL R. BOIX.[1], (Member, IEEE)

[1]Departamento de Electrónica y Electromagnetismo, Facultad de Física, Universidad de Sevilla, Av. Reina Mercedes s/n, Sevilla 41012, Spain (e-mail: armandof@us.es, medina@us.es, boix@us.es)
[2]Parts Laboratory Department, Alter Technology TÜV Nord S.A.U., 4 Thomas A. Edison Street, PCT Cartuja, Seville 41092, Spain (e-mail: aintzane.lujambio@altertechnology.com)
[3]Departamento de Física Aplicada II, ETSA, Av. Reina Mercedes s/n, Sevilla 41012, Spain (e-mail: martel@us.es)
[4]CIMITEC, Departament d'Enginyeria Electrònica, Universitat Autònoma de Barcelona, 08193 Bellaterra, Barcelona, Spain (e-mail: ferran.martin@uab.cat)

Corresponding author: Armando Fernández-Prieto (e-mail: armandof@us.es).

This work has been supported in part by the Spanish Ministerio de Economía y Competitividad with European Union FEDER Funds (contracts TEC2013-41913-P, TEC2016-75650-R, and TEC2017-84724-P), by the Spanish Junta de Andalucía (project P12-TIC-1435), and by Generalitat de Catalunya (contract 2014SGR-157).

ABSTRACT Two balanced-to-balanced planar diplexers based on magnetically coupled microstrip resonators are proposed in this paper. For the first prototype, each channel/differential-output is composed of a second order single-band balanced bandpass filter based on open-loop resonators. For the second diplexer example, the filters composing the differential outputs are fourth order and are implemented by means of folded stepped-impedance resonators. The design procedure for the differential response is quite straightforward, since it is based on the use of the well-known external quality factor and coupling coefficients concepts. Common-mode is inherently rejected thanks to the benefits of magnetic coupling, which precludes common-mode transmission over a wide frequency range. The proposed structure also offers a high level of channel-to-channel isolation. To demonstrate the usefulness of the proposed idea, the two prototypes are simulated, fabricated and measured. Good differential-mode and common-mode performance is observed in both examples. Simulations and measurements show good agreement.

INDEX TERMS Balanced-to-balanced diplexer, common-mode rejection, differential-mode, magnetic coupling, microstrip resonators.

I. INTRODUCTION

THE use of differential (or balanced) digital and analog circuits for information processing has increased in recent years [1]. When transmitting high-speed electrical signals, both the electromagnetic (EM) fields generated by the transmitted signals and the ground plane return current might cause electrical interference on adjacent circuits. Moreover, with the trend of digital systems to move to lower operating voltage, logic signal swing and noise margin also decrease, thus deteriorating the noise immunity of the digital system. Due to these and other reasons, differential signaling is becoming more and more popular in both digital and analog applications. Indeed, several common low-voltage communication standards (such as USB, Serial ATA or HDMI, among others) make use of differential signals. Note that, for the same operating voltage level, differential signals provide much lower return current on the ground plane, better immunity to noise, less electromagnetic interference (EMI) and less cross-talk when compared with conventional single-ended implementations. Also differential signals are not affected by external noise, which mainly couples to the common mode component of the total voltage. However, although ideal differential signals are supposed to solve all the above-mentioned problems, in a realistic scenario, where the circuit symmetry has been slightly broken or the applied signals present some level of time skew, the presence of common-mode (CM) noise is unavoidable. This CM noise is the source of most of the radiation and EMI problems. Hence,

This article has been accepted for publication in a future issue of this journal, but has not been fully edited. Content may change prior to final publication. Citation information: DOI 10.1109/ACCESS.2018.2820073, IEEE Access

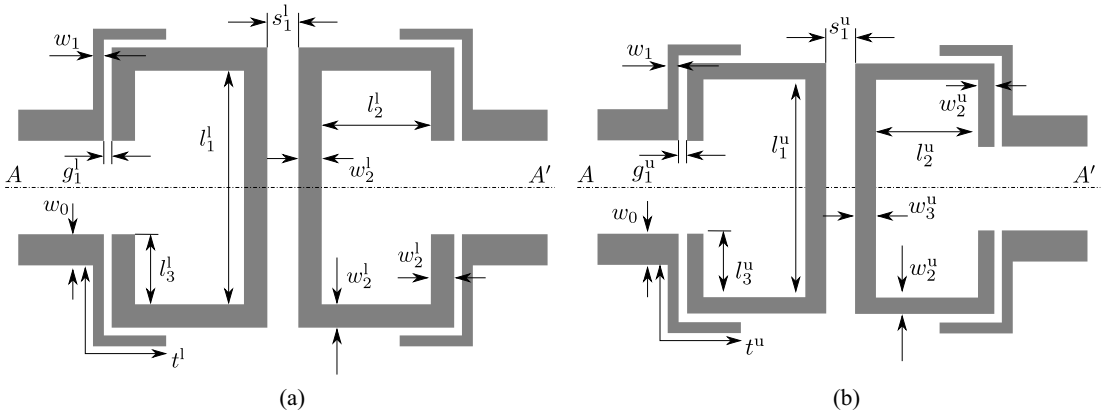

FIGURE 1. Layout of the balanced single-band bandpass filters proposed to perform the balanced diplexing operation. Dimensions (in mm) are: (a) lower-band filter: $l_1^l = 16.9$, $l_2^l = 4.9$. $l_3^l = 4$, $w_2^l = 0.8$, $s_1^l = 2$, $g_1^l = 0.2$, $t^l = 7.61$; **(b) upper-band filter:** $l_1^u = 13.5$, $l_2^u = 4$. $l_3^u = 2.3$, $w_2^u = 0.5$, $w_3^u = 0.8$ $s_1^u = 2$, $g_1^u = 0.2$ **and** $t^u = 4.67$**. Dimensions for the feeding structure (also in mm) are** $w_0 = 2.53$, $w_1 = 0.2$**.**

differential circuits should be designed in such a way that CM is rejected and, at the same time, the differential-mode (DM) signal is not perturbed, thus preserving its integrity within the frequency range of interest. In this context, many microwave differential (or balanced) devices have been proposed in the literature, including common-mode filters based on artificial differential-lines [2]–[12], balanced bandpass filters [6], [7], [13]–[26], power dividers / combiners [27]–[31], diplexers [32]–[42] and passive equalizers [43]. Among the aforementioned balanced devices, common-mode filters and balanced bandpass filters are, by far, the ones that have attracted more attention in the literature. However, much less research has been carried out in the area of microwave differential diplexers. Given the current trends towards multi-band systems, diplexers offer a very interesting solution to increase the compactness and to reduce the cost of RF front-ends.

Therefore, the design of balanced diplexers deserves more attention. To the authors' knowledge, two different kind of diplexers with differential operation have been proposed in the literature: (i) balun diplexers, and (ii) balanced diplexers. Balun diplexers are composed of a single-ended input port and two balanced output ports (or vice versa) [32]–[35]. In a balanced diplexer both input and output channels are differential in nature [34]–[39] (we will refer to this type of diplexers as *Balanced-to-Balanced* (B-B) diplexers). In all cases, the most common procedure to perform differential diplexing operation consists in the design of two different filters (single-ended or balanced) connected to a common input port (which, again, can be single-ended or balanced). Good DM transmission properties, high channel-to-channel isolation and weak CM transmission are simultaneously required. Several techniques have been used to accomplish the aforementioned goals to a greater or lesser extent. For example, the balun diplexers in [32], [33] make use of bandpass filters whose resonators have DM and CM resonance frequencies far apart from each other. The filters are connected to a common input by means of a T-junction, providing good DM and CM responses with high isolation. However, this configuration presents an intricate geometry, which complicates the design process. This idea was extended in [34] to design a balun diplexer and a balanced diplexer whose resonators require ground connection through via-holes. This feature introduces additional complexity in the design and manufacturing process. The same concept is used in [36] for the design of balanced diplexers, with the novelty of the introduction of transmission zeros (TZs) associated with the existence of mutual couplings between stub-loaded input/output lines. Although DM selectivity and isolation are good, CM suppression is poor due to the extra coupling path provided by the input/output lines. To solve this problem, the structure in [36] is modified in [37] by introducing shorted stubs along the resonators symmetry plane. The length of the stubs is adjusted so as to introduce a common-mode TZ at the center frequency of each channel passband. The main drawback of this technique is, once again, the requirement of using via holes. In [35], the use of hybrid microstrip/slotline resonators prevents CM transmission and allows for the design of balun and balanced diplexers with good DM performance and high isolation levels. However, in practical applications, ground planes without slots are preferred to reduce radiation losses and possible electromagnetic compatibility (EMC) issues. Very recently, the authors of this contribution have presented a B-B diplexer based on edge-coupled split ring resonators based filters [38]. This design provides both good DM and CM response with a very compact design, at the expense of being a complicated structure where a sophisticated excitation mechanism is required. Finally, two different B-B diplexers using Chebyshev responses are presented in [39] based on dual-mode resonators with magnetic coupling and microstrip-slotline coupling schemes. Although good performance within the passbands is obtained for both DM and CM, the proposed structures exhibit a relatively large electrical size. In addition, rather poor channel isolation is observed, and the structure with magnetic coupling suffers from CM resonances in the out-of-band region, thus

This article has been accepted for publication in a future issue of this journal, but has not been fully edited. Content may change prior to final publication. Citation information: DOI 10.1109/ACCESS.2018.2820073, IEEE Access

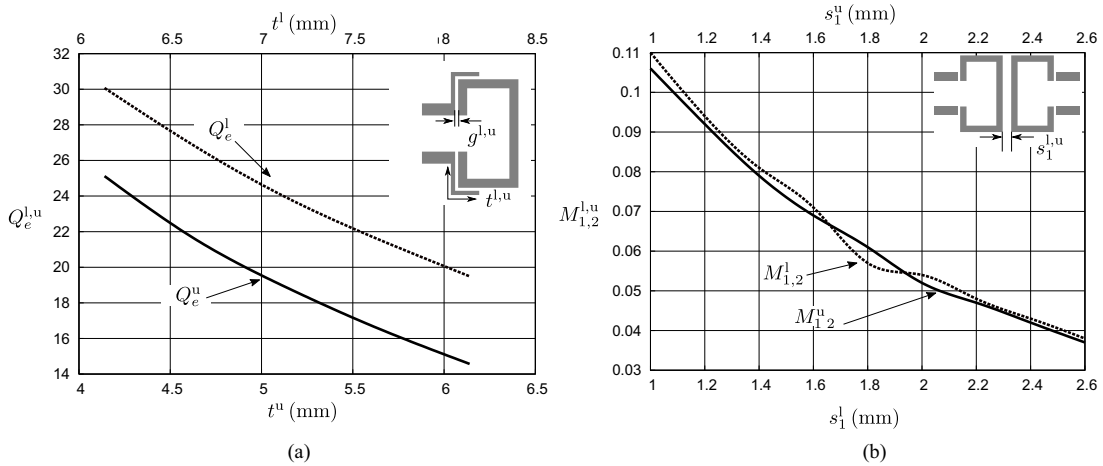

FIGURE 2. **(a) External quality factors for the lower (Q_e^{l}) and upper (Q_e^{u}) band balanced filters as a function of t^{l} and t^{u}, respectively. A fixed value of $g_1^{\mathrm{l}} = g_1^{\mathrm{u}} = 0.2$ mm has been chosen. (b) Coupling coefficients ($M_{1,2}^{\mathrm{l,u}}$) for the lower and upper band balanced filters as functions of s_1^{l} and s_1^{u}, respectively.**

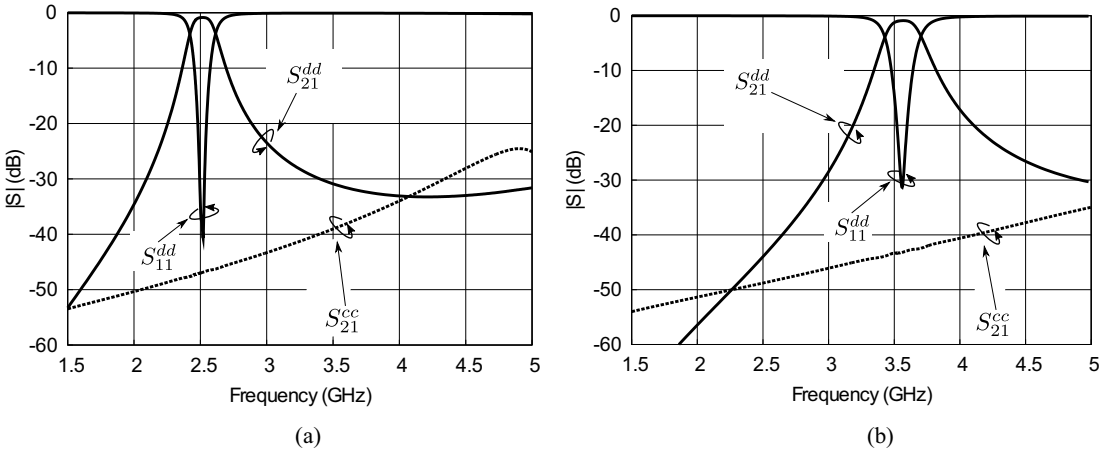

FIGURE 3. **Simulated DM and CM responses for (a) the lower bandpass filter and (b) the upper bandpass filter.**

degrading the CM performance in the upper frequency region of the spectrum. To end this section, it is worth mentioning that some works on balanced quad-band diplexers making use of the techniques mentioned above have recently been reported [40]–[42].

In a recent paper by some of the authors, it was demonstrated that the use of magnetically coupled open-loop or folded stepped-impedance resonators offers a very simple solution to implement single-band balanced bandpass filters with high CM suppression and excellent DM performance [19]. The electric nature of the CM coupling ensures an inherently poor CM transmission when magnetic coupling is used to generate the differential response. In the present paper two novel balanced diplexers are proposed which are based on open-loop (prototype I) and FSIRs (prototype II) balanced single-band bandpass filters. It will be shown how the use of a well-known design methodology [44] for coupled resonator filters makes it possible the fabrication of a compact and high-performance balanced diplexer by joining the two balanced filters to a common balanced input. The paper is organized as follows: in section II the first diplexer prototype, based on two second order coupled open-loop resonators balanced filters, is presented. The second prototype, based on a couple of fourth order coupled stepped-impedance resonators (FSIRs) balanced filters, is presented in section III. Finally, some conclusions are provided in section IV to summarize the advantages of the proposed approach.

II. PROTOTYPE I: BALANCED DIPLEXER BASED ON SECOND ORDER FILTERS

A. PROPOSED BALANCED BAND-PASS FILTERS

As it has been said in the introduction, the design of the B-B diplexers proposed in this contribution starts with the design of the two required balanced filters. Each filter is independently designed and connected to the same differential input port to obtain the differential diplexing operation. The layouts of the microstrip configurations used for the implementation of the filters [19] composing the balanced diplexer prototype I are shown in Fig. 1(a) and Fig. 1(b). In what follows, the superscripts "l" and "u" denote the lower- and

This article has been accepted for publication in a future issue of this journal, but has not been fully edited. Content may change prior to final publication. Citation information: DOI 10.1109/ACCESS.2018.2820073, IEEE Access

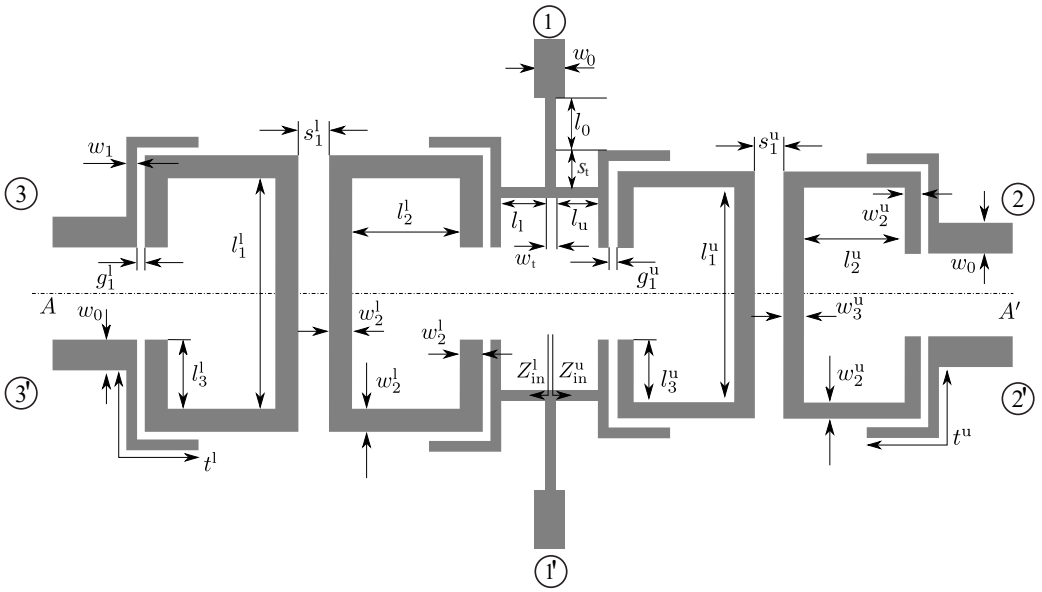

FIGURE 4. **Layout of the proposed balanced diplexer (not to scale). Final dimensions (in mm) for the T-junction are $w_0 = 2.53$ (corresponding to a 50 Ω line), $w_t = 0.2$, $l_0 = 1.8$, $s_t = 0$ (these three values have been set *a priori*), $l_l = 2.36$ and $l_u = 1.96$ (as it is explained in the text, these two values for the feeding length lines have been calculated to preserve the external quality factors of the isolated filters). The other dimensions are identical to those in Fig. 1(a) and Fig. 1(b).**

upper- DM passbands. Under DM operation, the symmetry plane, AA', in Fig. 1 behaves as a virtual short-circuit, thus forcing the coupling mechanism of this configuration to be mainly magnetic in nature. However, under CM operation AA' is a virtual open-circuit, which leads to electric coupling in this case. As it was proven in [19], these features make it possible to design balanced bandpass filters with good DM performance and an inherently strong CM rejection. This response is achieved because of the contrast between the achieved weak electric coupling (CM) and strong magnetic coupling (DM). Apart from strong CM suppression, high DM and CM isolation between channels is provided by the chosen solution. The design of the balanced filters in Fig. 1(a) and (b) can be easily carried out using the appropriate values of the coupling coefficients, M, and external quality factors, Q_e, according to the method explained in [44]. The values of M and Q_e depend on the DM filter specifications through the following well-known expressions [44]:

$$M_{i,i+1} = \frac{\Delta}{\sqrt{g_i g_{i+1}}}, \quad \text{for} \quad i = 1, \ldots, n-1 \qquad (1)$$

$$Q_{e1} = \frac{g_0 g_1}{\Delta} \qquad Q_{en} = \frac{g_n g_{n+1}}{\Delta} \quad , \qquad (2)$$

where n is the filter order, Δ is the fractional bandwidth and g_j ($j = 0, \ldots, n+1$) are the low-pass prototype element values for the filter response to be implemented. In the case at hand, two $n = 2$ Butterworth filters, with $\Delta^l = \Delta^u = 7\,\%$, and center frequencies $f_{0d}^l = 2.5\,\text{GHz}$, $f_{0d}^u = 3.5\,\text{GHz}$ are intended to be designed. The values of the corresponding low-pass prototype elements are $g_0 = g_3 = 1$ and $g_1 = g_2 = 1.4142$. Using these parameters and the required bandwidth, the theoretical values for $M_{1,2}$ and Q_e (the same for both bands in this particular case) can be computed using (1) and (2). This results in $M_{1,2}^l = M_{1,2}^u = M_{1,2} = 0.049$ and $Q_{e1}^l = Q_{e2}^l = Q_e^l = Q_{e1}^u = Q_{e2}^u = Q_e^u = 20.20$. The dielectric constant of the chosen substrate is $\varepsilon_r = 3.0$, its thickness $h = 1.016\,\text{mm}$ and the loss tangent $\tan\delta = 0.0022$.

Once the characteristics of the DM passbands have been selected, the following design step is to determine the dimensions of the resonators leading to the center frequencies f_{0d}^l and f_{0d}^u. These frequencies are mainly controlled by the total lengths of the resonators, which have to be close to half the guided wavelength at f_{0d}^l and f_{0d}^u (see Fig. 1(a) and Fig. 1(b) for dimensions). The fine adjustment of the dimensions is accurately accomplished with the help of an electromagnetic simulator (in our case, ADS-Momentum [45]). Next, the external quality factor, Q_e, and the coupling coefficient, $M_{1,2}$, required for each passband section are extracted by following the procedure reported in [44, Chap. 7]. For the lower DM passband Q_e^l mainly depends on the gap distance g_1^l and the length t^l (see Fig. 1(a)). Equivalently, Q_e^u can be tuned by properly selecting g_1^u and t^u. In order to facilitate the design process, in both filters the gap distance has been fixed to $g_1^l = g_1^u = 0.20\,\text{mm}$. The values of Q_e^l and Q_e^u are plotted in Fig. 2(a) as functions of t^l and t^u, respectively. From these curves, the required value of $Q_e = 20.20$ is obtained when $t^l = 8.0\,\text{mm}$ and $t^u = 4.67\,\text{mm}$. The value of $M_{1,2}^{l,u}$ is controlled by the gap distance between resonators, $s_1^{l,u}$. When two synchronous coupled resonators are weakly excited, the resonance frequency f_0 splits around f_0 into two different resonance frequencies, f_{p1} and f_{p2}. According to [44, Chap. 7], the coupling coefficient can be calculated from

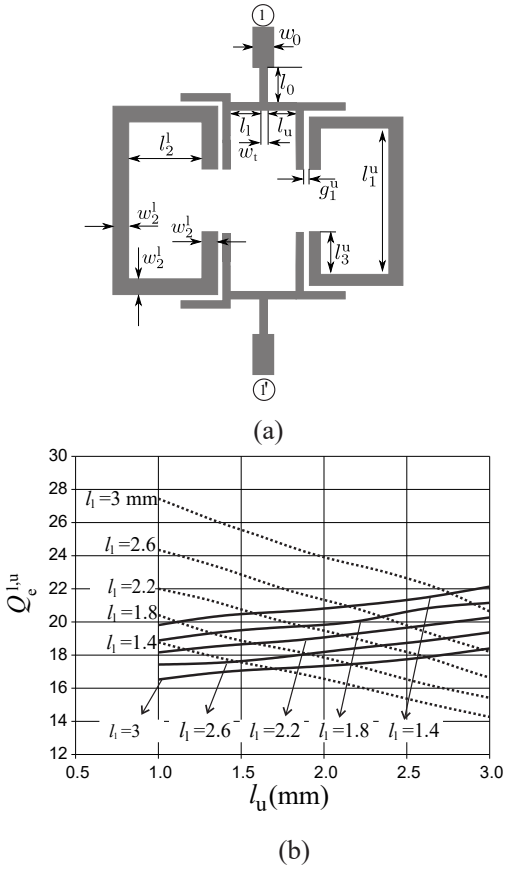

FIGURE 5. **(a) Structure used to determine $Q_e^{l,u}$. (b) Values of Q_e^u (dotted lines) and Q_e^l (solid lines) versus l_u using l_l as parameter. The remaining parameters are in the captions of Fig. 1 and Fig. 4.**

f_{p1} and f_{p2} by means of the expression:

$$M_{12} = \frac{f_{p1}^2 - f_{p2}^2}{f_{p1}^2 + f_{p2}^2}. \tag{3}$$

Using this method, design curves for $M_{1,2}^{l,u}$ as a function of s_1^l and s_1^u have been obtained and depicted in Fig. 2(b). In order to obtain the required coupling coefficient, $M_{1,2} = 0.049$, we can set $s_1^l = s_1^u = 2$ mm. The design process of both filters is now concluded. To verify that the design has been carried out correctly, the simulated differential- and common-mode responses of both filters are depicted in Fig. 3(a) and (b). The results reveal the strong CM rejection obtained with this configuration and the good DM performance.

B. BALANCED BAND-PASS FILTERS COMBINATION

If the balanced filters designed in subsection II.A are connected to a common differential input port, balanced diplexing operation can be performed. The proposed layout is shown in Fig. 4, where a T-junction is used to connect both filters. In this figure, Z_{in}^l and Z_{in}^u represent the input impedances of the lower and upper branches of the T-junction seen from the T-junction bifurcation. The key point when introducing the T-junction is that the external quality factors

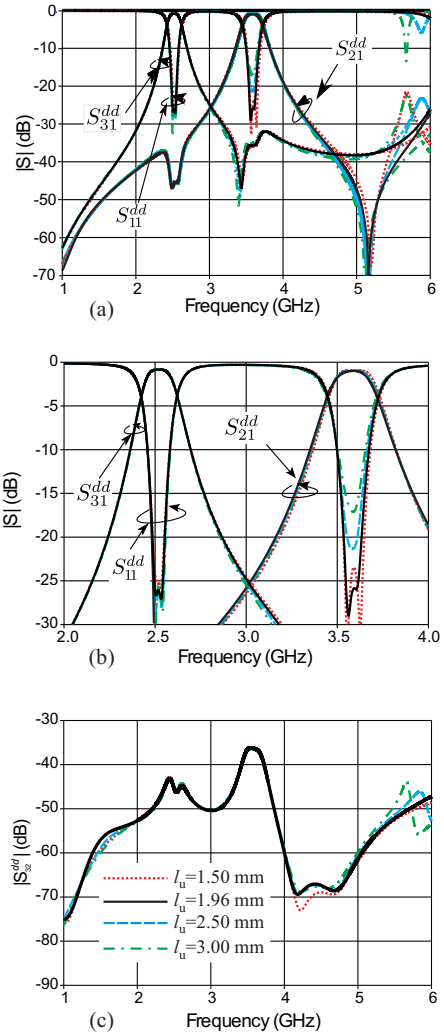

FIGURE 6. **DM response of the balanced diplexer for $l_l = 2.36$ mm, l_u varying from 1.5 to 3 mm. Black solid line corresponds to the final design value $l_u = 1.96$ mm. (a) Return loss ($|S_{11}^{dd}|$) and insertion loss of differential ports 2 ($|S_{21}^{dd}|$) and 3 ($|S_{31}^{dd}|$); (b) detailed view of the differential passbands; (c) DM isolation between the differential output ports ($|S_{32}^{dd}|$).**

at the filter inputs must be those imposed by the design specifications. The T-junction must be then designed to preserve the required external quality factors. This ensures low return loss level at both output channels (good signal matching). As it can be seen in Fig. 4, there are several dimensional parameters involved in the T-junction design. For simplicity, we have set the values of $l_0 = 1.8$ mm, $w_t = 0.2$ mm and $s_t = 0$. The lengths of the branch feeding lines, l_u and l_l, have been used as the adjustable parameters to fit the desired external quality factors. Fig. 5(a) shows the coupling structure with the T-junction used to calculate the external quality factors Q_e^u and Q_e^l by means of the procedure reported in [44, Chap. 7]. Note that, in contrast with the procedure followed in subsection II.A, where Q_e^u and Q_e^l are separately calculated, here we propose the simultaneous determination of the external quality factors. For such derivation, it has been

This article has been accepted for publication in a future issue of this journal, but has not been fully edited. Content may change prior to final publication. Citation information: DOI 10.1109/ACCESS.2018.2820073, IEEE Access

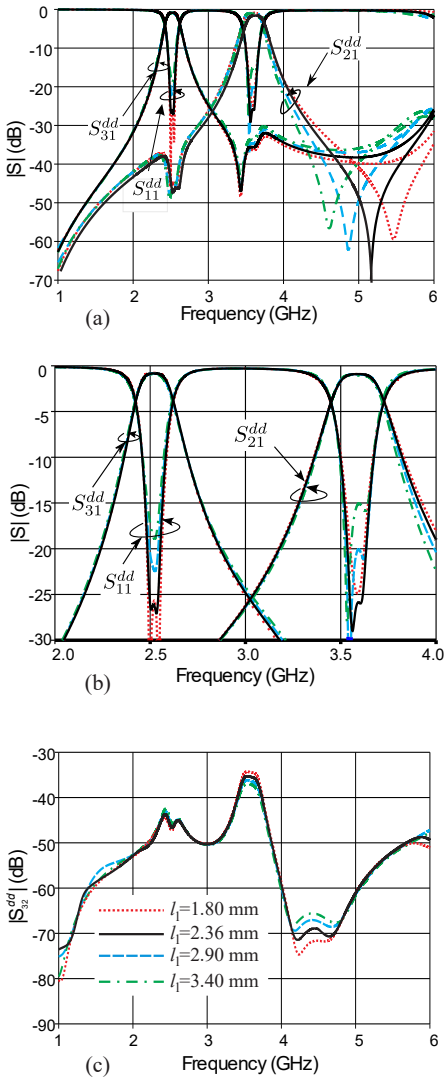

FIGURE 7. DM response of the balanced diplexer for $l_u = 1.96$ mm, l_l varying from 1.8 to 3.4 mm. Black solid line corresponds to the final design value $l_l = 2.36$ mm. (a) Return loss ($|S_{11}^{dd}|$) and insertion loss for differential ports 2 ($|S_{21}^{dd}|$) and 3 ($|S_{31}^{dd}|$); (b) detailed view of the differential passbands; (c) DM isolation between ports 2 and 3 ($|S_{32}^{dd}|$).

considered that, at f_{0d}^{l}, the upper-band resonator in Fig. 5(a) acts as a reactive load at the input of the lower-band resonator and vice versa. This provides a real and complete characterization of the input external quality factors of both channels. The design curves showing the behavior of $Q_e^{l,u}$ versus l_u using l_l as a parameter are depicted in Fig. 5(b). Although, as expected, Q_e^{u} (Q_e^{l}) exhibits a stronger dependence with l_u (l_l) than with l_l (l_u), for an accurate derivation of Q_e^{u} and Q_e^{l} both lengths must be considered. From Fig. 5(b), the values required to fulfill $Q_e^{u} = Q_e^{l}$ =20.2 are $l_l = 2.36$ mm and $l_u = 1.96$ mm.

In order to verify the validity of the method used to design the T-junction, Fig. 6 shows the simulated DM response of the diplexer for $l_l = 2.36$ mm by using l_u as sweep parameter. From Fig. 6(b) it can be seen that the lower band is well-matched for any value of l_u, whereas the upper band return loss is strongly dependent on l_u. The calculated value $l_u = 1.96$ mm provides the best return loss for the upper passband. The port-to-port isolation, $|S_{32}^{dd}|$, is depicted in Fig. 6(c). It can be seen that the dimensions of the T-junction barely affect the isolation level between the two channels. This level keeps better than 35 dB and with almost the same frequency response independently of l_u. This is an expected result, due to the separation between the two passbands. In Fig. 7 a similar study is carried out interchanging the roles of l_l and l_u (now $l_u = 1.96$ mm). This figure shows that the value of $l_l = 2.36$ mm provides the best matching for both bands. Note that this parameter can also be used to control the precise location of a transmission zero (TZ) existing around 5 GHz, if an adequate tradeoff between the position of this TZ and the matching level is attained. This TZ appears at the frequency at which $Z_{in}^{l} = 0\ \Omega$. At such frequency the signal will see a short circuit thus flowing towards the branch of the T-junction feeding the lower band channel. Then a TZ will appear at the upper band channel. Finally, the results for $|S_{32}^{dd}|$ shown in Fig. 7(c) confirm our hypothesis of good isolation between ports 2 and 3,independently of the dimensions of the T-junction.

In order to clarify the design process of the B-to-B diplexer proposed in this section, the following summary is given below:

1) The isolated filters are designed following the standard procedure well detailed in references [19] and [44].
2) A T-junction with some arbitrarily chosen dimensions (for w_t, l_0, l_l, l_u and s_t) is introduced.
3) There are several geometrical parameters defining the T-junction layout. Only two of those parameters have to be tuned to optimize the matching of the diplexer ports, since there are only two electrical parameters (the lower- and upper-band external quality factors) to be adjusted. Therefore, only the lengths of the branch feeding lines (l_l, l_u) are used as adjustable parameters to fit the required external quality factors at the input ports of the filters. The remaining geometrical parameters are not modified in this optimization process. This step ends the design of the proposed B-to-B diplexer.

C. EXPERIMENTAL RESULTS AND DISCUSSION

A prototype of the balanced diplexer in Fig. 4 has been fabricated using a LPKF Protolaser S machine and measured using the Agilent PNA-E8363B ANA with a N4420B test-set extension (four ports system). The simulated and measured DM and CM responses are shown in Fig. 8(a-d), and a photograph of the fabricated device is shown in Fig. 9. According to the plots in Fig. 8(a-d), the agreement between simulations and measurements is very good. The measured DM lower and upper passbands are centered at 2.51 GHz and 3.57 GHz, with an insertion loss (IL) level at the center frequencies of 1.14 dB and 1.21 dB, respectively.

The experimental fractional bandwidth is, as required, 7 % for both passbands. The measured DM isolation (Iso) is better

This article has been accepted for publication in a future issue of this journal, but has not been fully edited. Content may change prior to final publication. Citation information: DOI 10.1109/ACCESS.2018.2820073, IEEE Access

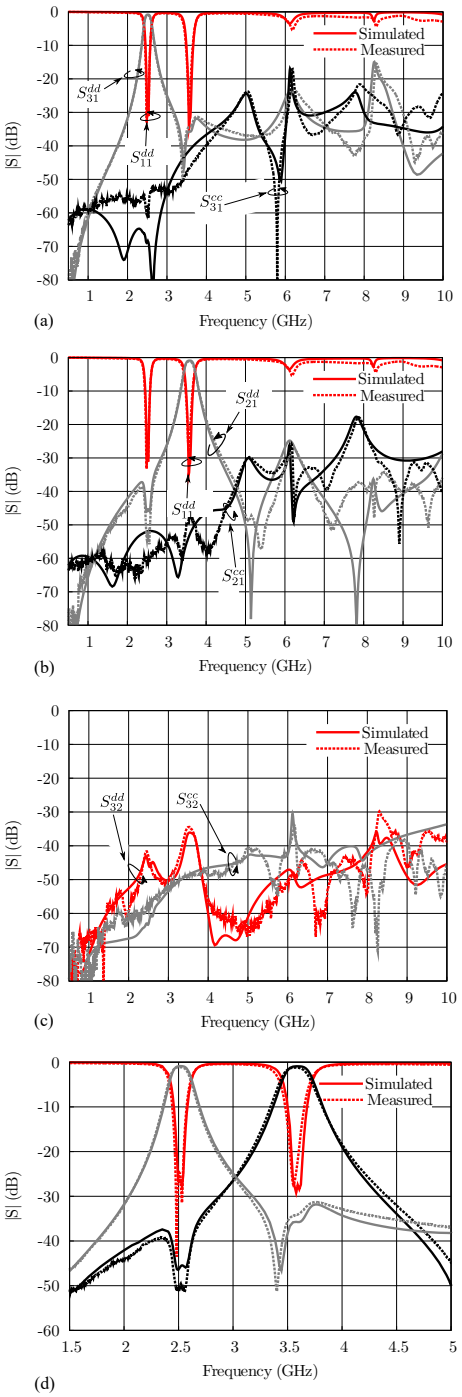

FIGURE 8. Simulated (solid lines) and measured (dotted lines) responses for the designed diplexer (see Fig. 4). (a) Lower band channel scattering parameters, (b) upper band channel scattering parameters, (c) differential- and common-mode isolation, and (d) detail of the differential passbands.

than 40 dB for the lower frequency channel and better than 33 dB for the upper one. In addition, the measured CM rejection is better than 50 dB and 48 dB for the lower and upper-band channels, respectively. Furthermore, concerning the out-of-band performance of the DM, a rejection better than 20 dB is appreciated over almost the whole frequency

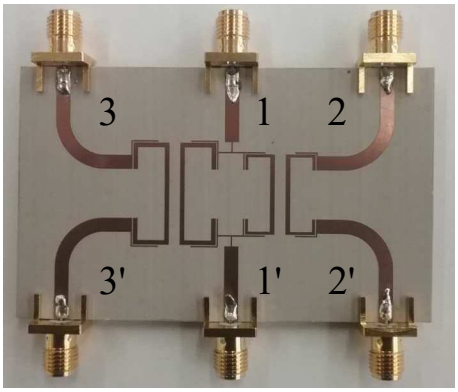

FIGURE 9. Photograph of the fabricated prototype whose scattering parameters are depicted in Fig. 8.

range up to 10 GHz (there is a transmission peak of about -15 dB at around 8.3 GHz). Concerning CM rejection, it is better than 15 dB in both channels until 10 GHz and better than 50 dB within the two differential pass-bands, leading to a high level of CMRR (as it will be seen in the forthcoming comparison table). Finally, CM and DM isolation are better than 30 dB until 10 GHz. This demonstrates that the diplexer provides a very good response not only within the differential passbands of both channels, but also in the out-of-band region, over a wide bandwidth, for all the relevant scattering parameters.

In order to illustrate the benefits of using magnetically coupled resonators for the design of balanced diplexers, a comparison with previous contributions is provided in Table I. From the data included in this table, it can be concluded that the balanced diplexer proposed in this paper exhibits a very competitive combination of common mode rejection ratio (CMRR) and size. These advantageous features have been highlighted in the table. Regarding the rest of electrical parameters, the presented structure is also very competitive. In addition, the structure is obtained by following a very simple design process, where no higher order filters or additional elements such as via-holes, defected ground structures or lumped/distributed components are needed. In spite of the simplicity of the design, a very good performance has been achieved for the diplexer operation.

III. PROTOTYPE II: BALANCED DIPLEXER BASED ON FOURTH ORDER FILTERS

A. FILTERS AND DIPLEXER DESIGN

The low-order balanced diplexer studied in the previous section has been shown to be very effective to divide a differential signal into two different channels (with good isolation between them) and, at the same time, to prevent CM transmission. However, it would be quite interesting to test if our proposal is suitable to operate when the two differential outputs must handle signals which are closer to each other in the frequency domain. For this, better filter selectivity is required for both channels. To achieve this goal, extra coupling paths can be introduced in the structure. This technique

This article has been accepted for publication in a future issue of this journal, but has not been fully edited. Content may change prior to final publication. Citation information: DOI 10.1109/ACCESS.2018.2820073, IEEE Access

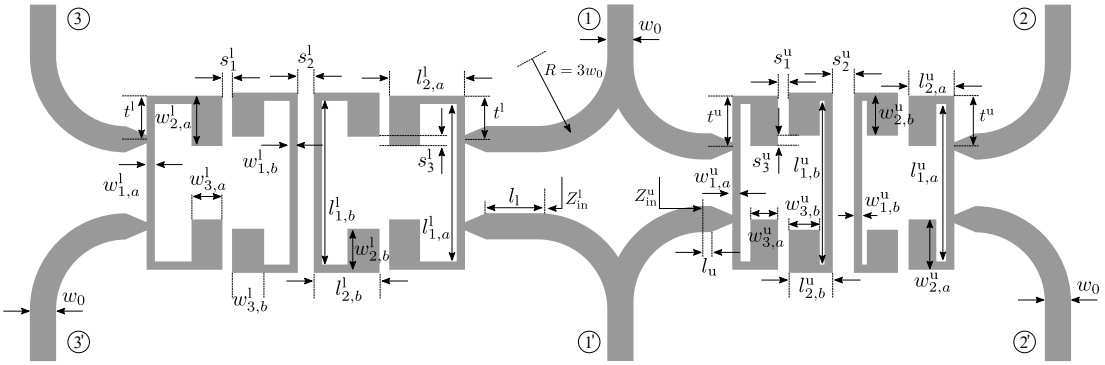

FIGURE 10. Layout of the proposed fourth order balanced diplexer (not to scale). Dimensions (in mm) are: (a) lower-band channel: $t^l = 4.2$, $w_{1,a}^l = 0.8$, $w_{2,a}^l = 4.86$, $w_{3,a}^l = 2.98$, $l_{1,a}^l = 15.2$, $l_{2,a}^l = 7.32$, $w_{1,b}^l = 0.8$, $w_{2,b}^l = 4.26$, $w_{3,b}^l = 3.1$, $l_{1,b}^l = 15.8$, $l_{2,b}^l = 6.35$, $s_1^l = 0.21$, $s_2^l = 1.54$, $s_3^l = 0.9$ and $l_l = 5$; (b) upper-band channel: $t^u = 4.1$, $w_{1,a}^u = 0.8$, $w_{2,a}^u = 4.86$, $w_{3,a}^u = 2.68$, $l_{1,a}^u = 15.2$, $l_{2,a}^u = 4.42$, $w_{1,b}^u = 0.8$, $w_{2,b}^u = 4.16$, $w_{3,b}^u = 3$, $l_{1,b}^u = 15.8$, $l_{2,b}^u = 4.25$, $s_1^u = 0.31$, $s_2^u = 2.04$, $s_3^u = 1$ and $l_u = 0.4$. Dimensions for the feeding structure (also in mm) are $w_0 = 2.53$, $R = 7.59$.

TABLE 1. Comparison with reported balanced and balun diplexers.

	Type	Area (λ_g^2)†	Differential-mode					Common-mode
			$f_{0d}^{l,u}$ (GHz)	f_{0d}^u/f_{0d}^l	3-dB $\Delta^{l,u}$(%)	IL $f_{0d}^{l,u}$ (dB)	Iso$^+$ (dB)	CMRR^{++} @$f_{0d}^{l,u}$ (dB)
[32]	U-B*	0.315	1 / 1.2	1.2	10.5 / 10.4	2.2 / 2.35	46.5 / 46.5	55 / 50
[33]	U-B	0.202	1.847 / 2.467	1.34	11.6 / 8.7	1.48 / 1.78	≈ 45 / 45	38.5 / 38.22
[34]	U-B	0.225	1.93 / 2.46	1.27	7.2 / 4.5	0.67 / 1.07	42.1 / 39.5	36.7 / 42.9
[34]	B-B	0.225	1.94 / 2.46	1.27	6.7 / 4.5	0.88 / 0.98	42.1 / 40.1	26.4 / 46.9
[35]	U-B	0.544	2.41 / 3.57	1.48	4.6 / 8.7	1.56 / 1.66	41.3 / 44.5	55.7 / 53.6
[35]	B-B**	0.550	2.45 / 3.55	1.45	6.7 / 8.2	1.95 / 2.11	39.5 / 44.5	50.2 / 47.7
[36]	B-B	0.099	2.46 / 3.65	1.48	8.1 / 4.9	1.5 / 2	33 / 42	28.5 / 30
[37]	B-B	N/A	2.45 / 3.6	1.47	6 / 3	1.3 / 1.8	≈ 35 / 55	≈ 56.7 / 48.2
[38]	B-B	0.046	1.47 / 2.19	1.49	11.5 / 7	0.94 / 2	43.3 / 40.0	39.06 / 42.8
[39]	B-B	0.342	1.87 / 2.26	1.21	9.6 / 8.0	1.56 / 2.05	25.07 / 25.07	57.0 / 54.4
Fig. 4	B-B	**0.094**	2.51 / 3.57	1.42	7 / 7	1.14 / 1.21	43.7 / 35.0	**57.1 / 49.1**
Fig. 10	B-B	**0.218**	**2.49 / 2.98**	**1.19**	15 / 10	1.15 / 1.54	35 / 33	**57.6 / 47.32**

† λ_g: Guided wavelength @ the lower-band frequency; * U-B: Unbalanced-to-balanced; ** B-B: Balanced-to-balanced; + Iso: Minimum DM Isolation within the passbands; ++ CMRR: Common-mode rejection ratio; N/A: substrate characteristics not provided.

allows for the introduction of several TZs at the expense of degrading CM rejection (CM finds in the extra coupling paths an alternative way to pass through the system). Thus, in this paper, in order to improve filters selectivity, a different strategy will be followed: the employment of higher order filters. Since the structures in this paper are very simple and the design procedure is well stablished, increasing the filters order is straightforward. Obviously, this will enhance filters selectivity. The layout of the new proposed diplexer (prototype II) is shown in Fig. 10. As in the previous example, the lower- and upper-frequency band channels are $33'$ and $22'$, respectively. Each filter involves two different resonators which have been denoted by subscripts "a" and "b". Comparing the layouts in Fig. 4 and Fig. 10, two important differences can be appreciated:

1) The filters in Fig. 10 are not capacitively excited but inductively excited. This is due to the fact that fourth order filters have two different coupling sections: an electric coupling section (between resonators "a-b" separated by $s_1^{l,u}$) and a magnetic coupling section (between resonators "b-b" separated by $s_2^{l,u}$). Since the excitation is carried out by the inductive region (strip of width $w_{1,a}^{l,u}$) of resonators "a", inductive excitation is more effective and simpler than capacitive excitation, as discussed, for instance, in [19]. However, the presence of at least one section with magnetic coupling in each filter ensures strong CM rejection, as it will be demonstrated next.
2) The resonators used in Fig. 10 are FSIRs, instead of open-loop resonators. This has been done wih two main targets. The first one is to achieve compactness. Since the filters of the B-B diplexer in this section require the use of more resonators, the use of FSIRs allows for a reasonably compact design when compared with the one obtained using open-loop resonators. Second, to demonstrate that the methodology used in the previous section can be employed with different kind of microstrip resonators. In this sense, the method is

quite general, as discussed in [44].

After these considerations, we are now in a position to define the characteristics of the differential passbands for the channels of the diplexer in Fig. 10: both filters will be of order $n = 4$, with Butterworth response, $\Delta^{\mathrm{l}} = 15\%$, $\Delta^{\mathrm{u}} = 10\,\%$, and center frequencies $f_{0d}^{\mathrm{l}} = 2.49\,\mathrm{GHz}$, $f_{0d}^{\mathrm{u}} = 2.98\,\mathrm{GHz}$. Note that the differential passband fractional bandwidths have been chosen to be different, in contrast with our previous example. According to (1) and (2), the required values of the coupling coefficients and external quality factors result to be: (i) lower channel $M_{1,2}^{\mathrm{l}} = M_{3,4}^{\mathrm{l}} = 0.13$, $M_{2,3}^{\mathrm{l}} = 0.081$, $Q_{e1}^{\mathrm{l}} = Q_{e4}^{\mathrm{l}} = Q_{e}^{\mathrm{l}} = 5.10$ and (ii) upper channel $M_{1,2}^{\mathrm{u}} = M_{3,4}^{\mathrm{u}} = 0.084$, $M_{2,3}^{\mathrm{u}} = 0.054$, $Q_{e1}^{\mathrm{u}} = Q_{e4}^{\mathrm{u}} = Q_{e}^{\mathrm{u}} = 7.654$. The low-pass prototype element values for the calculation of the external quality factors and coupling coefficients are $g_0 = g_5 = 1$, $g_1 = g_4 = 0.7654$ and $g_2 = g_3 = 1.8478$. The same substrate used to design and fabricate the prototype I is employed in this design. Design curves similar to those in Fig. 2(a) and (b) can be plotted to extract the required values of $M_{i,i+1}^{\mathrm{l,u}}$ and $Q_{e}^{\mathrm{l,u}}$. Such curves have not been included here in order to save some space and prevent writing a too long paper. Nevertheless, it is worth to clarify that $M_{1,2}^{\mathrm{l,u}}$ ($M_{3,4}^{\mathrm{l,u}}$) and $M_{2,3}^{\mathrm{l,u}}$ are controlled by $S_{1}^{\mathrm{l,u}}$ and $S_{2}^{\mathrm{l,u}}$, respectively, while $Q_{e}^{\mathrm{l,u}}$ are controlled by $t^{\mathrm{l,u}}$, respectively. Once the filters have been designed, both are connected to the common differential input $11'$ by means of a T-junction, whose branches are optimized in order to preserve the required external quality factors. Curves similar to those in Fig. 5 can be plotted in order to find the correct values of l_{l} and l_{u}, although they have not been included here for the sake of brevity. The final dimensions of the B-B diplexer presented in this section are shown in the caption of Fig. 10.

B. EXPERIMENTAL RESULTS AND DISCUSSIONS

The diplexer in Fig. 10 has been simulated, fabricated and measured. The results are plotted in Fig. 11, where good agreement between simulations and measurements is found. The measured center frequencies (DM) and FBWs result to be $f_{0d}^{\mathrm{l}} = 2.49\,\mathrm{GHz}$, $f_{0d}^{\mathrm{u}} = 2.98\,\mathrm{GHz}$, $\Delta^{\mathrm{l}} = 15\%$, $\Delta^{\mathrm{u}} = 10\,\%$, respectively. The measured IL at the center frequencies is 1.15 dB (lower channel) and 1.54 dB (upper channel). When compared with the response in Fig. 8, channels roll-off is greater in this new design (better filters selectivity). DM isolation is well below 30 dB in the whole considered frequency range. Out-of-band rejection is also better than 30 dB practically until 10 GHz, except for a small transmission peak in channel $33'$ at about 9.1 GHz (still better than 20 dB). Regarding CM results, Fig. 11 reveals very strong rejection level in both channels (expected from magnetic coupling). CM suppression is larger than 50 dB and 45 dB for the lower and upper band, respectively. Moreover, CM rejection is better than 30 dB in the whole frequency range for both channels, except for a transmission peak of -15 dB in channel $22'$ at approximately 7 GHz. CM isolation is better than 40 dB until 10 GHz.

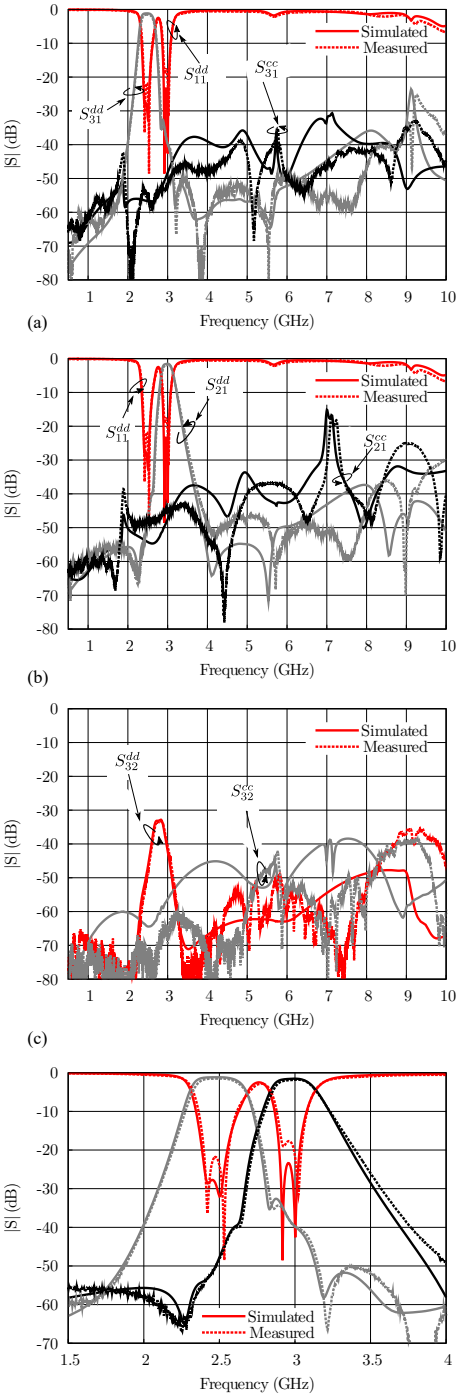

FIGURE 11. Simulated (solid lines) and measured (dotted lines) responses for the designed diplexer (see Fig. 10). (a) Lower band channel scattering parameters, (b) upper band channel scattering parameters, (c) differential- and common-mode isolation, and (d) detail of the differential passbands.

In brief, the proposed diplexer provides very good performance in terms of DM signal quality transmission and CM rejection. No interaction is observed between output channels notwithstanding the proximity between them. In order to demonstrate the benefits of the B-B diplexer within this

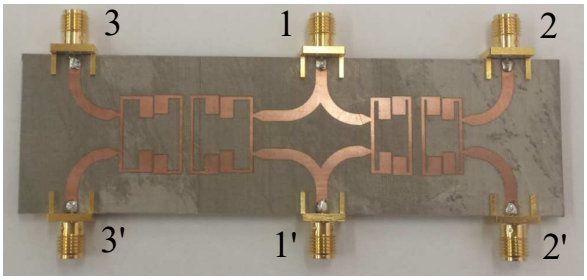

FIGURE 12. Photograph of the fabricated fourth order prototype.

section, it has been compared with other contributions in Table I. According to this table, the diplexer seems to be quite competitive in terms of CMRR, compactness (in spite of the order $n = 4$), and differential passbands proximity (our proposal provides the lowest value of $f_{0d}^{\mathrm{u}}/f_{0d}^{\mathrm{l}}$). A photograph of the fabricated prototype is depicted in Fig. 12.

IV. CONCLUSIONS

In this paper, two new balanced-to-balanced diplexers are presented in microstrip technology. Prototype I is composed of two balanced bandpass filters based on magnetically coupled open-loop resonators. Prototype II is based on two balanced bandpass filters designed using magnetically coupled stepped-impedade resonators. The design process in both cases is simple and straightforward. Basically, it consists in designing each filter independently, with their desired performances, and then joining them to the same differential input by means of a T-shaped connecting transmission-line path. The length of each arm of the T-junction must be tuned to provide a good level of return loss in the two passbands. Design curves can be generated from electromagnetic simulations taking into account the presence of the two resonators. This tuning process can be easily achieved with low computational cost. Measured results confirm the benefits of the proposed idea. Finally, when compared with previous contributions, prototype I offers one of the highest level of compactness and common-mode rejection ratio, while still being very competitive in terms of the other relevant electrical parameters. Prototype II provides the lowest ratio between center frequencies while conserving a competitive compactness in spite of the high-order filters used in the design. Good roll-off is observed in each channel for this prototype without the need of using complex transfer functions.

REFERENCES

[1] W. R. Eisenstant, B. Stengel, and B. M. Thompson, *Microwave Differential Circuit Design Using Mixed-Mode S-parameters*, Artech House, Boston, 2006.

[2] W.-T. Liu, C.-H. Tsai, T.-W. Han and T.-L. Wu, "An embedded common-mode suppression filter for GHz differential signals using periodic defected ground plane," IEEE Microw. Wireless Compon. Lett., vol. 18, no. 4, pp. 248–250, Apr. 2008.

[3] S.-J. Wu, C.-H. Tsai, T.-L. Wu and T. Itoh, "A novel wideband common-mode suppression filter for gigahertz differential signals using coupled patterned ground structure," IEEE Trans. Microw. Theory Techn., vol. 57, no. 4, pp. 848–855, Apr. 2009.

[4] C.-H. Tsai and T.-L. Wu, "A broadband and miniaturized common-mode filter for gigahertz differential signals based on negative-permittivity metamaterials," IEEE Trans. Microw. Theory Techn., vol. 58, no. 1, pp. 195–202, Jan. 2010.

[5] A. Fernández-Prieto, J. Martel, J. S. Hong, F. Medina, S. Qian and F. Mesa, "Differential transmission line for common-mode suppression using double side MIC technology," in Proc. of the 41st European Microw. Conf. (EuMC), pp. 631–634, Manchester (England, UK), Oct. 2011.

[6] J. Naqui, A. Fernández-Prieto, M. Durán-Sindreu, F. Mesa, J. Martel, F. Medina, and F. Martín, "Common mode suppression in microstrip differential lines by means of complementary split ring resonators: theory and applications," IEEE Trans. Microw. Theory Techn., vol. 60. no. 10, pp. 3023–3033, Oct. 2012.

[7] A. Fernández-Prieto, J. Martel, F. Medina, F. Mesa, S. Qian, J.-S. Hong, J. Naqui, and F. Martín, "Dual-band differential filter using broadband common-mode rejection artificial transmission line," Prog. in Electromag. Research (PIER), vol. 139, pp. 779–797, Apr. 2013.

[8] T.-W. Weng, C.-H. Tai, C.-H. Chen, D.-H. Han and T.-L. Wu "Synthesis model and design of a common-mode bandstop filter (CM-BSF) with all pass characteristics for high speed differential signals," IEEE Trans. Microw. Theory Techn., vol. 62, no. 8, pp. 1647–1656, Aug. 2014.

[9] G.-H. Shiue, C.-M. Hsu, C.-L. Lou and C.-F. Su, "A comprehensive investigation of a common-mode filter for gigahertz differential signals using quarter-wave resonators," IEEE Trans. Compon., Packag., Manufac. Technol., vol. 4. no. 1, pp. 134–144, Jan. 2014.

[10] P. Vélez, J. Bonache and F. Martín, "Differential microstrip lines with common-mode suppression based on electromagnetic bandgaps," IEEE Antennas Wireless Propag. Lett., vol. 18, pp. 40–43, Jan. 2015.

[11] A. Fernández-Prieto, S. Qian, J.-S. Hong, J. Martel, F. Medina, F. Mesa, J. Naqui, and F. Martín, "Common-mode suppression for balanced bandpass filters in multilayer liquid crystal polymer technology" IET Microw. Antennas Propag., vol. 9, no. 12, pp. 1249–1253, Sept. 2015.

[12] J. Martel, A. Fernández-Prieto, A. Lujambio, F. Medina, F. Mesa, and R. R. Boix, "Differential lines for common-mode suppression based in hybrid microstrip/CPW technology" IEEE Microw. Wireless Compon. Lett., vol. 27, no. 1, pp. 13–15, Jan. 2017.

[13] A. K. Horestani, M. Durán-Sindreu, J. Naqui, C. Fumeaux, and F. Martín, "S-shaped complementary split ring resonators and their application to compact differential bandpass filters with common-mode suppression," IEEE Microw. Wireless Compon. Lett., vol. 24, no. 3, pp. 149–151, March 2014.

[14] J. Shi and Q. Xue, "Balanced bandpass filters using center-loaded half-wavelength resonators," IEEE Trans. Microw. Theory Techn., vol. 58, no. 4, pp. 970–977, April 2010.

[15] P. Vélez, J. Naqui, A. Fernández-Prieto, M. Durán-Sindreu, J. Bonache, J. Martel, F. Medina, and F. Martín, "Differential bandpass filter with common-mode suppression based on open split ring resonators and open complementary split ring resonators," IEEE Microw. Wireless Compon. Lett., vol. 23, no. 1, pp. 22–24, Jan. 2013.

[16] C.-H. Wu, C.-H. Wang, and C. H. Chen, "Stopband-extended balanced bandpass filter using coupled stepped-impedance resonators," IEEE Microw. Wireless Compon. Lett., vol. 17, no. 7, pp. 507–509, July 2007.

[17] S.-C. Lin and C.-Y. Yeh, "Stopband-extended balanced filters using both $\lambda/4$ and $\lambda/2$ SIRswith common-mode suppression and improved selectivity," Prog. in Electromag. Research (PIER), vol. 128, pp. 215–228, May 2012.

[18] H. Wang, K.-W. Tam, S.-K. Ho, W. Kang, and W. Wu, "Short-ended self-coupled ring resonator and its application for balanced filter design," IEEE Microw. Wireless Compon. Lett., vol. 24, no. 5, pp. 312–314, May 2014.

[19] A. Fernández-Prieto, A. Lujambio, J. Martel, F. Medina, F. Mesa, and R. Boix, "Simple and compact balanced bandpass filters based on magnetically coupled resonators," IEEE Trans. Microw. Theory Techn., vol. 63, no. 6, pp. 1843–1853, June 2015.

[20] J. Shi and Q. Xue, "Novel balanced dual-band bandpass filter using coupled stepped impedance-resonators," IEEE Microw. Wireless Compon. Lett., vol. 20, no. 1, pp. 19–21, Jan. 2010.

[21] C.-H. Lee, C.-I.-G. Hsu, and C.-C. Hsu, "Balanced dual-band BPF with stub-loaded SIRs for common-mode suppression," IEEE Microw. Wireless Compon. Lett., vol. 20. no. 2, pp. 70–72, Feb. 2010.

[22] Y.-H. Cho and S.-W. Yun, "Design of balanced dual-band bandpass filters using asymmetrical coupled lines," IEEE Trans. Microw. Theory Techn., vol. 61, no. 8, pp. 2814–2820, Aug. 2013.

[23] F. Wei, Y.-J. Guo, P.-Y. Qin, and X.-W. Shi, "Compact balanced dual- and tri-band bandpass filters based on stub loaded resonators," IEEE Microw. Wireless Compon. Lett., vol. 25. no. 2, pp. 76–78, Feb. 2015.

[24] Y. Shen, H. Wang, W. Kang, and W Wu, "Dual-band SIW differential bandpass filter with improved common-mode suppression," IEEE Microw. Wireless Compon. Lett., vol. 25. no. 2, pp. 100–102, Feb. 2015.

[25] F. Wei, P.-Y. Qin, Y. J. Guo, C. Ding, and X. W. Shi, "Compact balanced dual- and tri-band BPFs based on coupled complementary split-ring resonators (C-CSRR)," IEEE Microw. Wireless Compon. Lett., vol. 26, no. 2, pp. 107–109, Feb. 2016.

[26] F. Bagci, A. Fernández-Prieto, A. Lujambio, J. Martel, J. Bernal and F. Medina, "Compact balanced dual-band bandpass filter based on modified coupled-embedded resonators," IEEE Microw. Wireless Compon. Lett., vol. 27, no. 1, pp. 31–33, Jan. 2017.

[27] B. Xia, L.-S. Wu, and J.-F. Mao, "A new balanced-to-balanced power divider/combiner," IEEE Trans. Microw. Theory Techn., vol. 60, no. 9, pp. 2791–2798, Sep. 2012.

[28] B. Xia, L.-S. Wu, S.-W. Ren, and J.-F. Mao, "A balanced-to-balanced power divider with arbitrary power division," IEEE Trans. Microw. Theory Techn., vol. 61, no. 8, pp. 2831–2840, Aug. 2013.

[29] L.-S. Wu, Y.-X. Guo, and J.-F. Mao, "Balanced-to-balanced Gysel power divider with bandpass filtering response," IEEE Trans. Microw. Theory Techn., vol. 61, no. 12, pp. 4052–4062, Dec. 2013.

[30] W. Feng, H. Zhu, W. Che, and Q. Xue, "Wideband in-phase and out-of-phase balanced power dividing and combining networks," IEEE Trans. Microw. Theory Techn., vol. 62, no. 5, pp. 1192–1202, May 2014.

[31] P. Vélez, M. Durán-Sindreu, A. Fernández-Prieto, J. Bonache, F. Medina and F. Martín, "Compact dual-band differential power splitter with common-mode suppression and filtering capability based on differential-mode composite right/left-handed transmission-line metamaterials," IEEE Antennas Wireless Propag. Lett., vol. 13, pp. 536–539, March 2014.

[32] C.-H. Wu, C.-H. Wang, and C.-H. Chen, "A novel balanced-to-unbalanced diplexer based on four-port balanced-to-balanced bandpass filter," in Proc. of 38th European Microw. Conf., Amsterdam (The Netherlands), pp. 28–31, 2008.

[33] Q. Xue, J. Shi, and J.-X. Chen, "Unbalanced-to-balanced and balanced-to-unbalanced diplexer with high selectivity and common-mode suppression," IEEE Trans. Microw. Theory Techn., vol. 59, no. 11, pp. 2848–2855, Nov. 2011.

[34] C. H. Lee, C. I. G. Hsu, and P. H. Wen, "Balanced and balun diplexers designed using center-grounded uniform-impedance resonators," Microw. Opt. Technol. Lett., vol. 56, no. 3, pp. 555–559, March 2014.

[35] P.-H. Weng, C.-I.-G. Hsu, C.-H. Lee, and H.-H. Chen, "Design of balanced and balun diplexers using stepped-impedance slot-line resonators," Journal of Electromagnetic Waves and Applications, vol. 28, no. 6, pp. 700–715, Feb. 2014.

[36] Y. Zhou, H.-W. Wei, and Y. Zhao, "Compact balanced-to-balanced microstrip diplexer with high isolation and common-mode suppression," IEEE Microw. Wireless Compon. Lett., vol. 24, no. 3, pp. 143–145, March 2014.

[37] H. Deng, Y. Zhao, Y. Fu, Y. He, and X. Zhao, "High selectivity and CM suppression microstrip balanced BPF and balanced-to-balanced diplexer," Journal of Electromagnetic Waves and Applications, vol. 27, no. 8, pp. 1047–1058, May 2013.

[38] A. Fernández-Prieto, A. Lujambio, F. Martín, J. Martel, F. Medina, and R. R. Boix, "Compact Balanced-to-Balanced Diplexer Based on Split-Ring Resonators Balanced Bandpass Filters," IEEE Microw. Wireless Compon. Lett., in press.

[39] X. Guo, L. Zhu and W. Wu "Balanced Diplexers Based on Inner-Coupled Dual-Mode Structures With Intrinsic Common-Mode Suppression," IEEE Access, vol. 5, pp. 26774-26782, Dec. 2017.

[40] H. L. Chan, C. H. Lee, and C. I. G. Hsu, "Balanced dual-band diplexer design using microstrip and slot-line resonators," in Proc. of 2015 Asia-Pacific Microw. Conf. (APMC), Nanjing (China), 2015, pp. 1–3.

[41] C. H. Lee, C. I. G. Hsu, S. X. Wu, and P. H. Wen, "Balanced quad-band diplexer with wide common-mode suppression and high differential-mode isolation," IET Microwaves, Antennas & Propag., vol. 10, no. 6, pp. 599–603, Apr. 2016.

[42] W. Jiang, Y. Huang, T. Wang, Y. Peng, and G. Wang, "Microstrip balanced quad-channel diplexer using dual-open/short-stub loaded resonator," in Proc. of 2016 IEEE MTT-S Int. Microw. Symp., San Francisco (CA, USA), pp. 1–3, 2016.

[43] C.-Y. Hsiao, and T.-L. Wu, "A novel dual-function circuit combining high-speed differential equalizer and common-mode filter with an additional zero," IEEE Microw. Wireless Compon. Lett., vol. 24, no. 9, pp. 617–619, Sep. 2014.

[44] J.-S. Hong, *Microstrip Filters for RF/Microwave Applications*, Second Edition, New York, Wiley 2011.

[45] ADS-Momentum, Keysight Technologies, http://www.keysight.com, accessed July 2017.

ARMANDO FERNÁNDEZ-PRIETO (S'11-M'14) was born in Ceuta, Spain, in September 1981. He received the Licenciado and Ph.D. degrees in physics from the University of Seville, Seville, Spain, in 2007 and 2013, respectively. He is currently involved with post-doctoral research with the Microwaves Group, University of Seville. His research interests focus on printed passive microwave components and metamaterials. Dr. Fernández-Prieto is a reviewer for the IEEE TRANSACTIONS ON MICROWAVE THEORY AND TECHNIQUES and IEEE Access, as well as for many other journals.

AINTZANE LUJAMBIO was born in San Sebastián (Guipúzcoa), Spain, in 1982. She received the Telecommunication Engineering degree and Ph.D. degree in communication technologies from the Public University of Navarre, Navarre, Spain, in 2006 and 2014, respectively. She has worked with the Microwaves Group, University of Seville. She has collaborated on several research projects supported by the Spanish Government and the European Commission. She is currently working as a test engineer at the EEE parts laboratory in Alter technology TÜV Nord. Her research interests include algorithms for microwave applications, inverse-scattering synthesis methods, passive microwave filters, and couplers.

JESÚS MARTEL (M'08-SM'15) received the Licenciado and Doctor degrees in physics from the University of Seville, Seville, Spain, in 1989 and 1996, respectively. Since 1990, he has performed research with the Microwave Group, University of Seville. In 1992, he joined the Department of Applied Physics II, University of Seville, where, in 2000, he became an Associate Professor, and in 2010, Head of the department. His current research interest is focused on the numerical analysis of planar transmission lines, the modeling of planar microstrip discontinuities, the design of passive microwave circuits, microwave measurements, and artificial media.

This article has been accepted for publication in a future issue of this journal, but has not been fully edited. Content may change prior to final publication. Citation information: DOI 10.1109/ACCESS.2018.2820073, IEEE Access

FRANCISCO MEDINA (M'90-SM'01-F'10) was born in Puerto Real, Cádiz, Spain, in November 1960. He received the Licenciado and Doctor degrees in physics from the University of Seville, Seville, Spain, in 1983 and 1987 respectively. He is currently a Professor of electromagnetism with the Department of Electronics and Electromagnetism, University of Seville, and Head of the Microwaves Group. He has coauthored more than 135 journal papers and book chapters, as well as more than 270 conference contributions. He is member of the Editorial Board of three technical journals. His research interests include analytical and numerical methods for planar structures, anisotropic materials, and artificial media modeling. Prof. Medina is a reviewer for about 45 IEEE, IET, AIP, and IoP journals. He has been member of the Technical Program Committees (TPCs) of a number of local and international leading conferences.

FERRAN MARTÍN (M'04-SM'08-F'12) was born in Barakaldo (Vizcaya), Spain in 1965. He received the B.S. Degree in Physics from the Universitat Autònoma de Barcelona (UAB) in 1988 and the PhD degree in 1992. From 1994 up to 2006 he was Associate Professor in Electronics at the Departament d'Enginyeria Electrònica, (Universitat Autònoma de Barcelona), and since 2007 he is Full Professor of Electronics. In recent years, he has been involved in different research activities including modelling and simulation of electron devices for high frequency applications, millimeter wave and THz generation systems, and the application of electromagnetic bandgaps to microwave and millimeter wave circuits. He is now very active in the field of metamaterials and their application to the miniaturization and optimization of microwave circuits and antennas. He is the head of the Microwave Engineering, Metamaterials and Antennas Group (GEMMA Group) at UAB, and director of CIMITEC, a research Center on Metamaterials supported by TECNIO (Generalitat de Catalunya). He has organized several international events related to metamaterials, including Workshops at the IEEE International Microwave Symposium (years 2005 and 2007) and European Microwave Conference (2009), and the Fifth International Congress on Advanced Electromagnetic Materials in Microwaves and Optics (Metamaterials 2011), where he has acted as chair of the Local Organizing Committee. He has acted as Guest Editor for three Special Issues on Metamaterials in three International Journals. He has authored and coauthored over 500 technical conference, letter, journal papers and book chapters, he is co-author of the book on Metamaterials entitled Metamaterials with Negative Parameters: Theory, Design and Microwave Applications (John Wiley Sons Inc. 2008), author of the book Artificial Transmission Lines for RF and Microwave Applications (John Wiley Sons Inc. 2015), and he has generated 16 PhDs. Ferran Martín has filed several patents on metamaterials and has headed several Development Contracts. Prof. Martín is a member of the IEEE Microwave Theory and Techniques Society (IEEE MTT-S). He is reviewer of the IEEE Transactions on Microwave Theory and Techniques and IEEE Microwave and Wireless Components Letters, among many other journals, and he serves as member of the Editorial Board of IET Microwaves, Antennas and Propagation and International Journal of RF and Microwave Computer-Aided Engineering. He is also a member of the Technical Committees of the European Microwave Conference (EuMC) and International Congress on Advanced Electromagnetic Materials in Microwaves and Optics (Metamaterials). Among his distinctions, Ferran Martín has received the 2006 Duran Farell Prize for Technological Research, he holds the Parc de Recerca UAB â Santander Technology Transfer Chair, and he has been the recipient of two ICREA ACADEMIA Awards (calls 2008 and 2013). He is Fellow of the IEEE since 2012 and Fellow of the IET since 2016.

RAFAEL R. BOIX (M'96) received the Licenciado and Doctor degrees in physics from the University of Seville, Seville, Spain, in 1985 and 1990, respectively. Since 1986, he has been with the Electronics and Electromagnetism Department, University of Seville, where he became a Tenured Professor in 2010. His current research interests focus on the efficient numerical analysis of periodic planar multilayered structures with applications to the design of frequency-selective surfaces and reflectarray/transmitarray antennas.